Supplementary Information

Light Scattering Study of Algal Floc Growth and Structure: Alum vs. Polymeric Plant-Derived Flocculant

Temitope Orimolade[a], Ngoc-Tram Le[a], Lyle Trimble[a], Bandaru V. Ramarao[b], and Sitaraman Krishnan[a,*]

[a]Department of Chemical & Biomolecular Engineering, Clarkson University, 8 Clarkson Avenue, Potsdam, New York 13699, USA

[b]Department of Chemical Engineering, SUNY College of Environmental Science & Forestry, 1 Forestry Drive, Syracuse, New York 13210, USA

*Corresponding author. Email: skrishna@clarkson.edu, Phone: +1 315 268 6661

Contents

S1 *Moringa oleifera* seed proteins

The low molecular weight, high charge-density cationic proteins from *Moringa oleifera* seeds, specifically MO2 and Mo-CBP3 (a 2S albumin), are effective flocculants for negatively charged particles. Their high arginine content, approximately 11.7%, significantly enhances this activity (see Table S1).

Table S1: Amino acid compositions of *M. oleifera* proteins

	MO2		**CBP3**	
Amino acid	#	%	#	%
Alanine	2	3.33	11	6.75
Cysteine	2	3.33	8	4.91
Aspartic acid	1	1.67	8	4.91
Glutamic acid	0	0.00	11	6.75
Phenylalanine	1	1.67	3	1.84
Glycine	5	8.33	6	3.68
Histidine	1	1.67	2	1.23
Isoleucine	2	3.33	6	3.68
Lysine	0	0.00	1	0.61
Leucine	3	5.00	15	9.20
Methionine	1	1.67	4	2.45
Asparagine	2	3.33	4	2.45
Proline	7	11.67	11	6.75
Glutamine	15	25.00	25	15.34
Arginine	7	11.67	19	11.66
Serine	4	6.67	8	4.91
Threonine	2	3.33	7	4.29
Valine	4	6.67	11	6.75
Tryptophan	0	0.00	1	0.61
Tyrosine	1	1.67	2	1.23
Total	60		163	
Molecular wt. (g/mol)	6782		18756	
Theoretical pI	11.61		7.55	

The amino acid sequence of the MO2 proteins is,[1]

> QGPGRQPDFQ RCGQQLRNIS PPQRCPSLRQ AVQLTHQQQG QVGPQQVRQM YRVASNIPST

and that of the 2S albumin CBP3 chitin-binding protein is,[2]

MAKLTLLLAT LALLVLLANA SIYRTTVELD EEPDDNQQQR CRHQFQTQQR LRACQRVIRR WSQGGGPMED VEDEIDETDE IEEVVEPDQA RRPPTLQRCC RQLRNVSPFC RCPSLRQAVQ SAQQQQGQVG PQQVGHMYRV ASRIPAICNL QPMRCPFRQQ QSS

The isoelectric point of MO2 is about 11.6. Both proteins are rich in glutamine (≈ 25.0% in MO2 and 15.3% in CBP3) and share a common glutamine-rich peptide sequence (QQQGQVG-PQQV) (highlighted in blue). They also contain significant amounts of nonpolar proline (approximately 11.7% in MO2 and 6.8% in CBP3).

S2 Properties of *M. oleifera* seed extract

Fig. S1: Photographs of (a) whole, (b) dehusked, and (c) powdered *Moringa oleifera* seeds, along with (d) the aqueous extract.

While powdered *M. oleifera* seeds are effective as flocculants, their use can increase organic matter in treated water, potentially promoting microorganism growth.[3] The seeds contain about 40% oils, 40% proteins, and 10% carbohydrates.[4] Deoiling the seeds or extracting the active flocculant can reduce the organic matter added during treatment. Several studies have explored extracting coagulation-active proteins using aqueous salt solutions.[5–7] Ndabigengesere et al.[5] found that only water extracts of *M. oleifera* seeds possess coagulation activity, while extracts using petroleum ether, hexane, chloroform, acetone, and methanol do not. Oladoja et al.[8] extracted seed proteins using aqueous NaCl solution, precipitated them with ammonium sulfate, and found that the precipitate, combined with soil (sand and clay), was an effective flocculant for *M. aeruginosa*, although a large amount of ammonium sulfate—six times the seed mass—was required in processing the seeds. Camacho et al.[9] studied the effectiveness of *M. oleifera* seed powders in three forms for cyanobacteria removal: untreated seed powder, oil-extracted using propane at 30 °C and 80 bar (reducing oil content by 94%), and oil-extracted using 95% ethanol (reducing oil content by 76%). They found that low-turbidity waters required the extraction of the active ingredient for effective turbidity reduction, which was not necessary for high-turbidity water. Madrona et

al.[10] compared the flocculation activity of *M. oleifera* proteins extracted using various KCl concentrations down to 0.01 M. Best results were with 1 M KCl, likely due to increased ionic strength enhancing protein concentration in the extract via the salting-in mechanism.[7,11] In this study, *M. oleifera seeds* were deoiled using 95% ethanol, and the seed proteins were extracted in 1 M aqueous NaCl solution.

Spectroscopic determination of M. oleifera protein concentration

Standard solutions of bovine serum albumin (BSA) with nominal concentrations of 0, 2, 4, 6, and 8 g/L were prepared by serial dilution of a 10 g/L BSA solution in aqueous NaCl (9 g/L). Their UV-vis spectra were recorded [see Fig. S2(a)]. The absorbance peak near 280 nm increased linearly with protein concentration up to about 6 g/L (data not shown). The BSA concentrations were corrected using the 280-nm absorbance and the known extinction coefficient of 0.667 $(\text{mg/mL})^{-1}\text{cm}^{-1}$.[12]

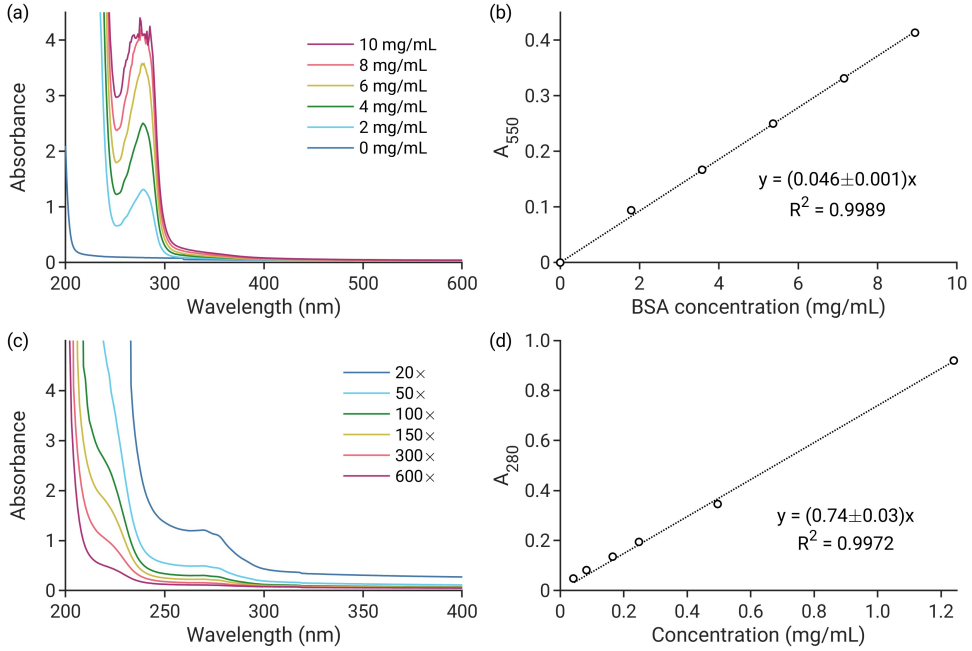

Fig. S2: (a) UV-vis spectra of BSA solutions in 0.9% aqueous NaCl with nominal concentrations ranging from 0 to 10 mg/mL protein. (b) Absorbance at 550 nm of BSA solution (1 mL) and Biuret reagent (4 mL). (c) UV-vis spectra of *M. oleifera* seed extracts in 1 M aqueous NaCl at various dilutions. (d) Absorbance at 280 nm of the *M. oliefera* extracts as a function of concentration (in BSA equivalents).

Next, a Biuret assay was conducted by adding 4 mL of Biuret reagent (Protein Assay Reagent M262, VWR) to 1 mL of each BSA standard, followed by vortexing and a 20-min incubation at room temperature. Absorbance at 550 nm was measured, with 9 g/L saline as the blank.

The plot of A_{550} vs. BSA concentration showed good linearity [see Fig. S2(b)], yielding an extinction coefficient ε_{550} of 0.046 ± 0.001 $(\mathrm{mg/mL})^{-1}\mathrm{cm}^{-1}$.

The Biuret assay was also applied to 1 mL of neat *M. oleifera* seed extract with 4 mL of Biuret reagent. The BSA equivalent concentration was derived from the calibration curve [Fig. S2(b)], resulting in 16 ± 2 mg/mL in the deoiled *Moringa* seed extract (DMSE).

Finally, by measuring the absorbance of diluted *M. oleifera* seed extract in 1 M NaCl solution, an extinction coefficient ε_{280} of 0.74 $(\mathrm{mg/mL})^{-1}\mathrm{cm}^{-1}$ for the *M. oleifera* protein was determined [Fig. S2(c) and (d)]. This coefficient could be used to calculate protein concentration in *M. oleifera* extracts from a single absorbance measurement at 280 nm, following suitable dilution.

Surface tension of M. oleifera seed extract

Fig. S3 shows the effect of *M. oleifera* protein concentration (in BSA equivalents) on the surface tension of the solution. The dependence of surface tension, γ (mN/m), on concentration, c (g/L), could be empirically fitted to an equation of the form:

$$\gamma = \gamma_0 - p_1 \ln\left(1 + p_2 c\right) \tag{S1}$$

The values of the parameters γ_0, p_1, and p_2 are shown in Fig. S3.

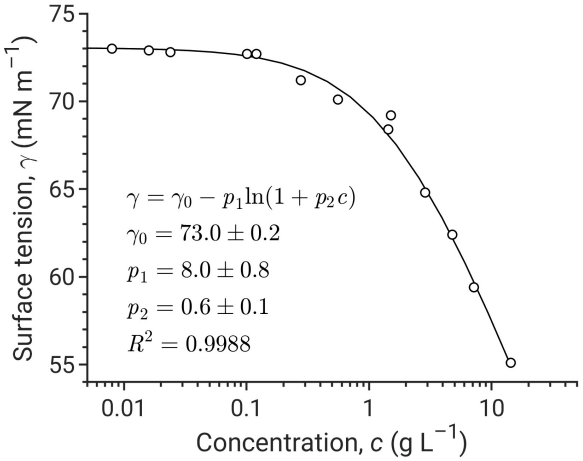

Fig. S3: Surface tension versus concentration of the active ingredient in the extracts of deoiled *M. oleifera* seeds in 1 M aqueous NaCl at 23.5 °C.

S3 Size distribution in *M. aeruginosa* suspensions at different cell concentrations

Fig. S4 shows the size distribution of *M. aeruginosa* cells in suspensions of three different concentrations. Flocculation of the cells is evident even without adding a flocculant. The flocs remained relatively stable at 70 rpm. In the 200 μg/L Chl *a* suspension, the flocs stabilized after a small decrease in size, whereas those in the 800 μg/L Chl *a* suspension showed a slight increase due to shear-induced aggregation.

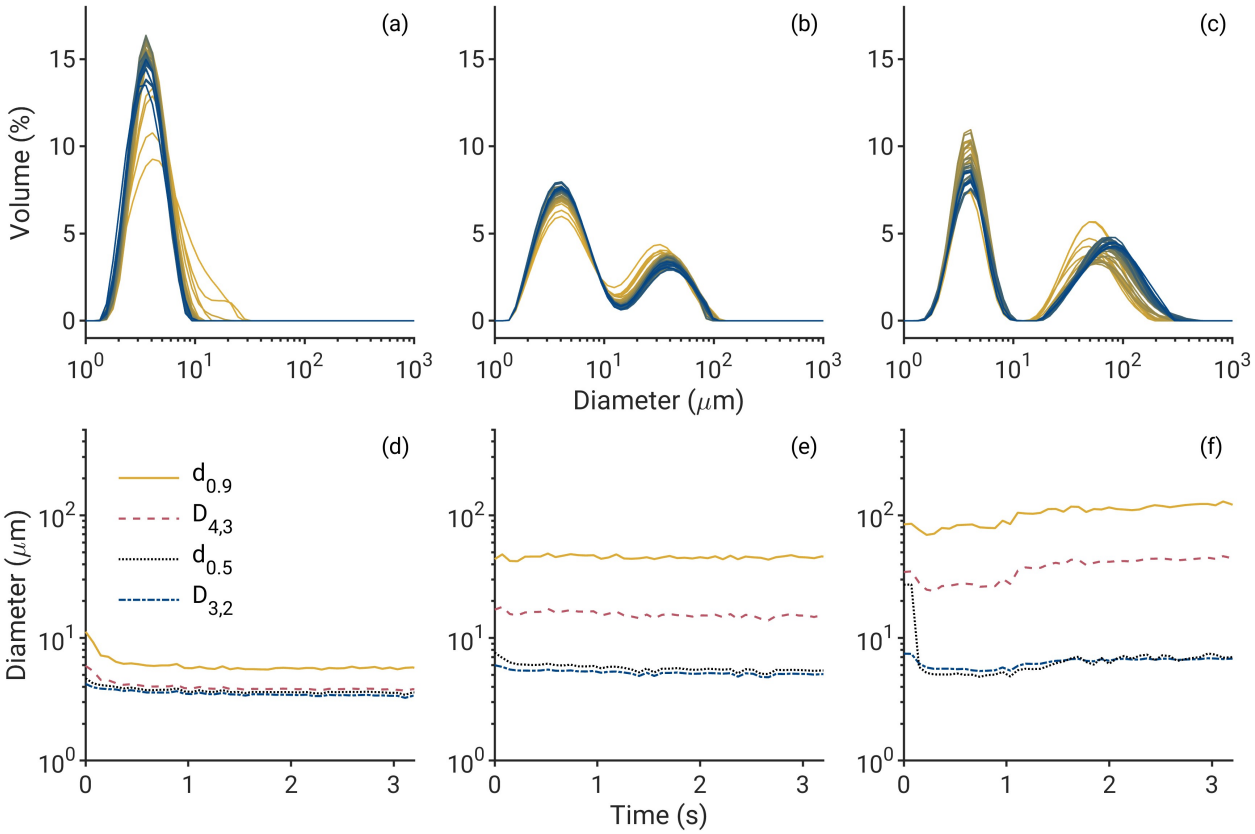

Fig. S4: (a–c) Volume distribution of *M. aeruginosa* suspensions at cell densities of 200, 400, and 800 μg/L Chl *a*. Each panel shows data from 43 measurements taken approximately every ≈74 s. Shades of yellow indicate earlier measurements, while blue represents later times. (d–f) Time evolution of $d_{0.9}$, $D_{4,3}$, $D_{3,2}$, and $d_{0.5}$. Stirring speed was 70 rpm during measurement.

Fig. S5 shows the obscuration data for *M. aeruginosa* suspensions at various cell concentrations. The obscuration levels ranged from approximately 3% to 20%, falling within the recommended range for the instrument used.[13]

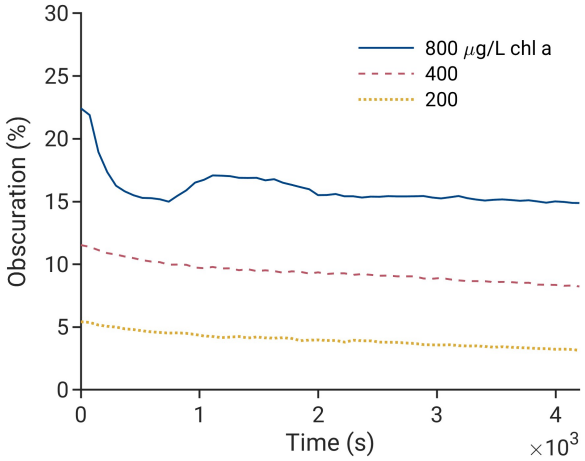

Fig. S5: Obscuration of *M. aeruginosa* cell suspensions at 800, 400, and 200 μg/L Chl a concentrations.

S4 Efficiencies of scattering using Mie theory

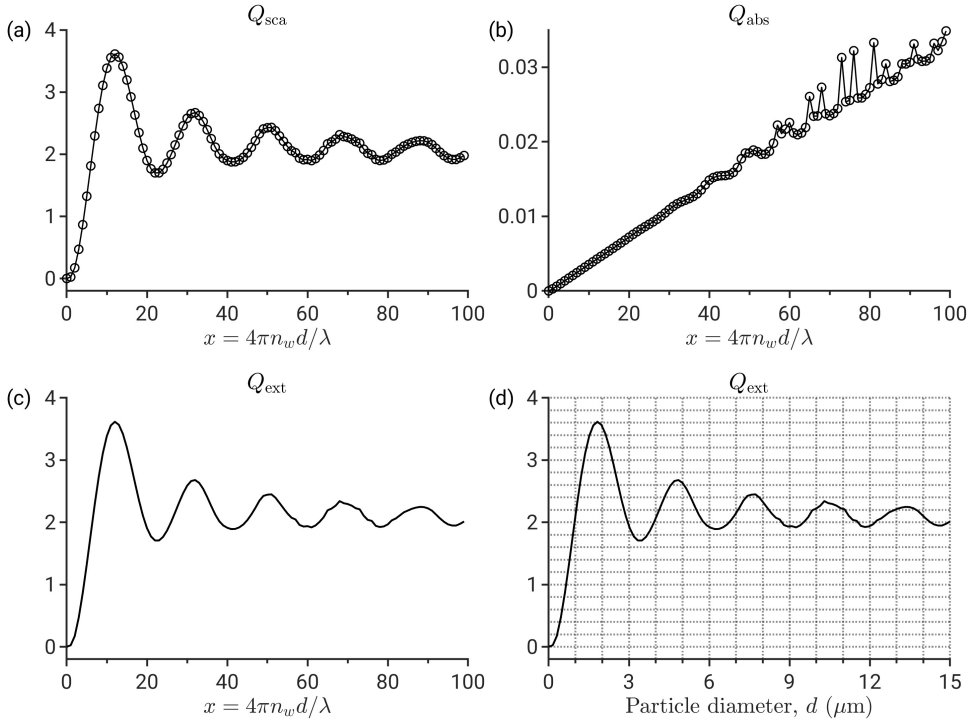

Fig. S6: Efficiencies of scattering (Q_{sca}), absorption (Q_{abs}), and extinction (Q_{ext}) versus particle size, calculated using Mie theory for particles with a refractive index of $m = 1.17 + 0.0001i$, where m is the complex refractive index of the algal cells relative to water.

Fig. S6 shows the efficiencies of scattering (Q_{sca}), absorption (Q_{abs}), and extinction (Q_{ext}) calculated using this value of particle refractive index. The variable, x, in Fig. S6(a–c) is

the product of the wavenumber, k, of light in the ambient medium (water) and the particle diameter, d.

$$k = \frac{4\pi}{\lambda_w} \tag{S2}$$

where λ_w is the wavelength in the water, given by the ratio of the light wavelength in the air ($\lambda = 633$ nm), and the refractive index of water ($n_w \approx 1.33$).

S5 Jar test procedure and results

Jar tests were conducted on 100 mL of *M. aeruginosa* cell suspensions in a 250 mL beaker, stirred magnetically at 60 rpm for 1 h. Alum was tested at concentrations ranging from 100 to 400 mg/L, while the *M. oleifera* extract was tested at concentrations ranging from 2 to 8 mL/L. After mixing, a 10-mL sample was transferred to a glass vial and allowed to settle for 1 h. Microscopic analysis using a Nikon Eclipse L200N optical microscope was performed on samples collected from the settled suspension. Representative results of the jar tests are shown in Fig. S7.

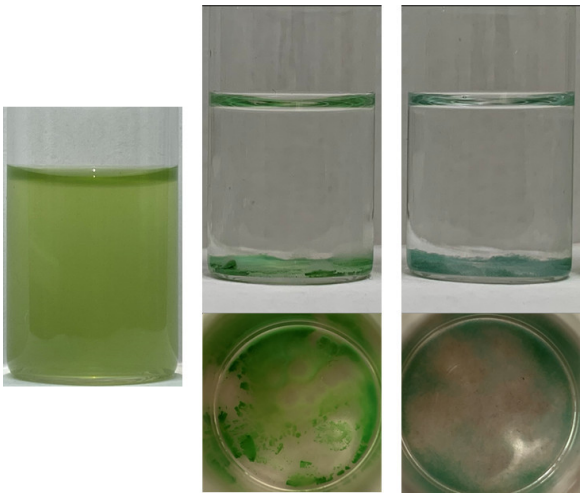

Fig. S7: Photographs of *Microcystis aeruginosa* cell suspension at 800 µg/L Chl *a*: (left) without flocculant, (center) with 2 mL/L DMSE, and (right) with 0.1 g/L alum suspension. Front and top views of flocculated suspensions.

S6 Floc size evolution of *M. aeruginosa* with alum

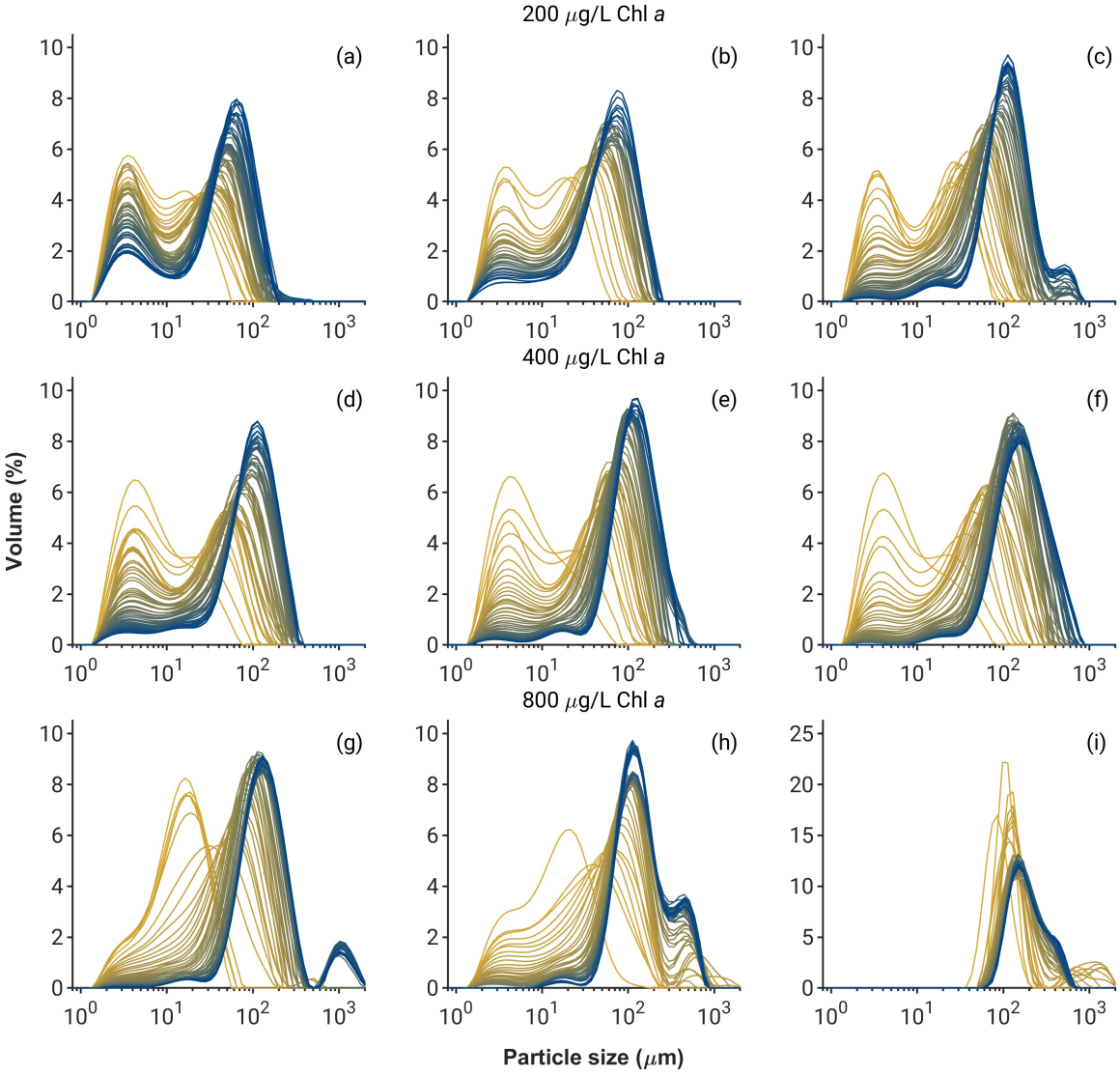

Fig. S8: Time evolution of the volume distribution of flocs in *M. aeruginosa* cell suspensions in the presence of alum. Top row: 200 μg/L Chl *a*. Middle row: 400 μg/L Chl *a*. Bottom row: 800 μg/L Chl *a*. Left column: 0.1 g/L alum. Center column: 0.2 g/L alum. Right column: 0.4 g/L alum. Size distribution measurement was made every ≈74 s. Stirring speed = 70 rpm.

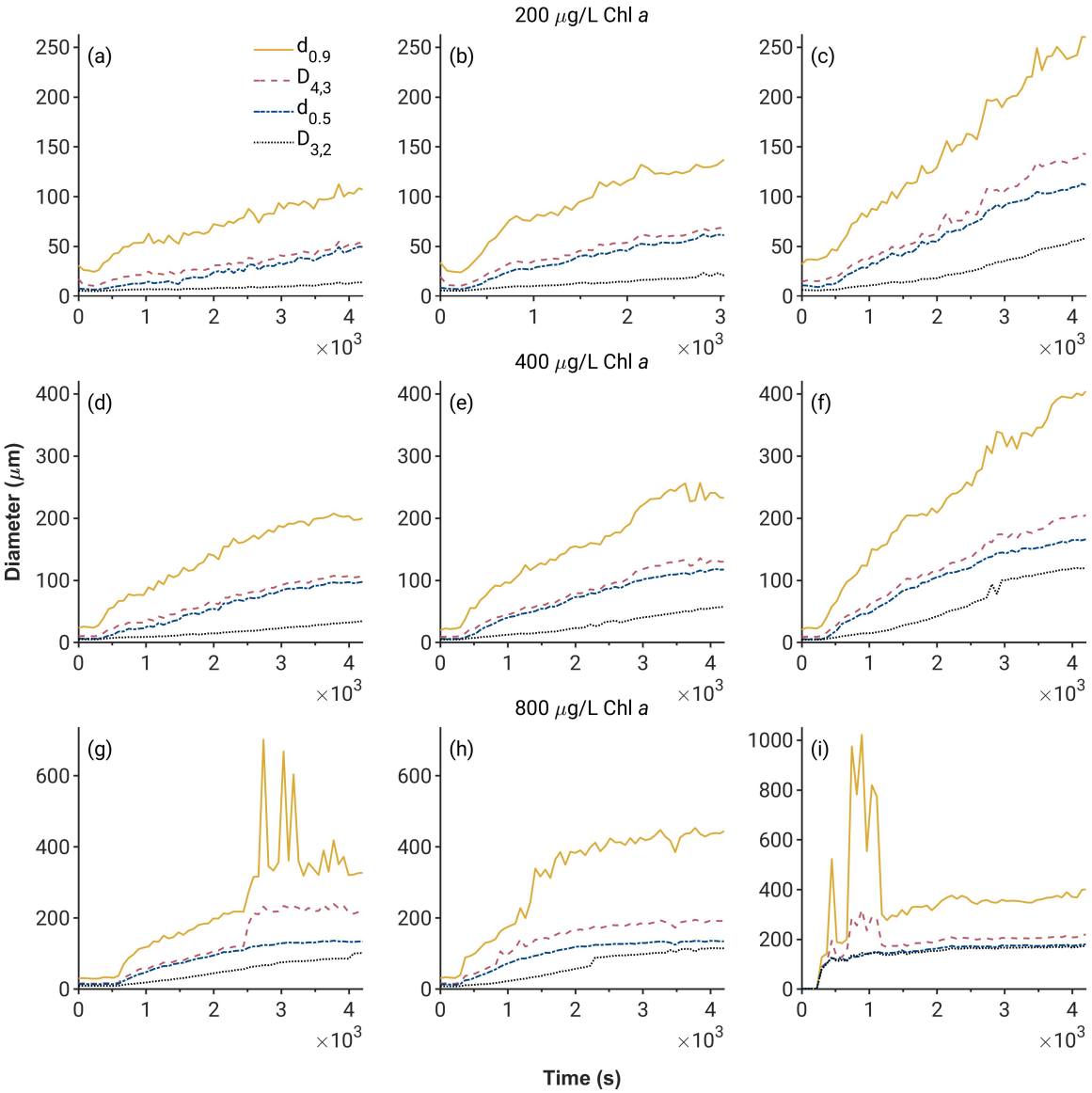

Fig. S9: Time evolution of floc diameters in *M. aeruginosa* cell suspensions in the presence of alum. Top row: 200 μg/L Chl *a*. Middle row: 400 μg/L Chl *a*. Bottom row: 800 μg/L Chl *a*. Left column: 0.1 g/L alum. Center column: 0.2 g/L alum. Right column: 0.4 g/L alum. Stirring speed = 70 rpm.

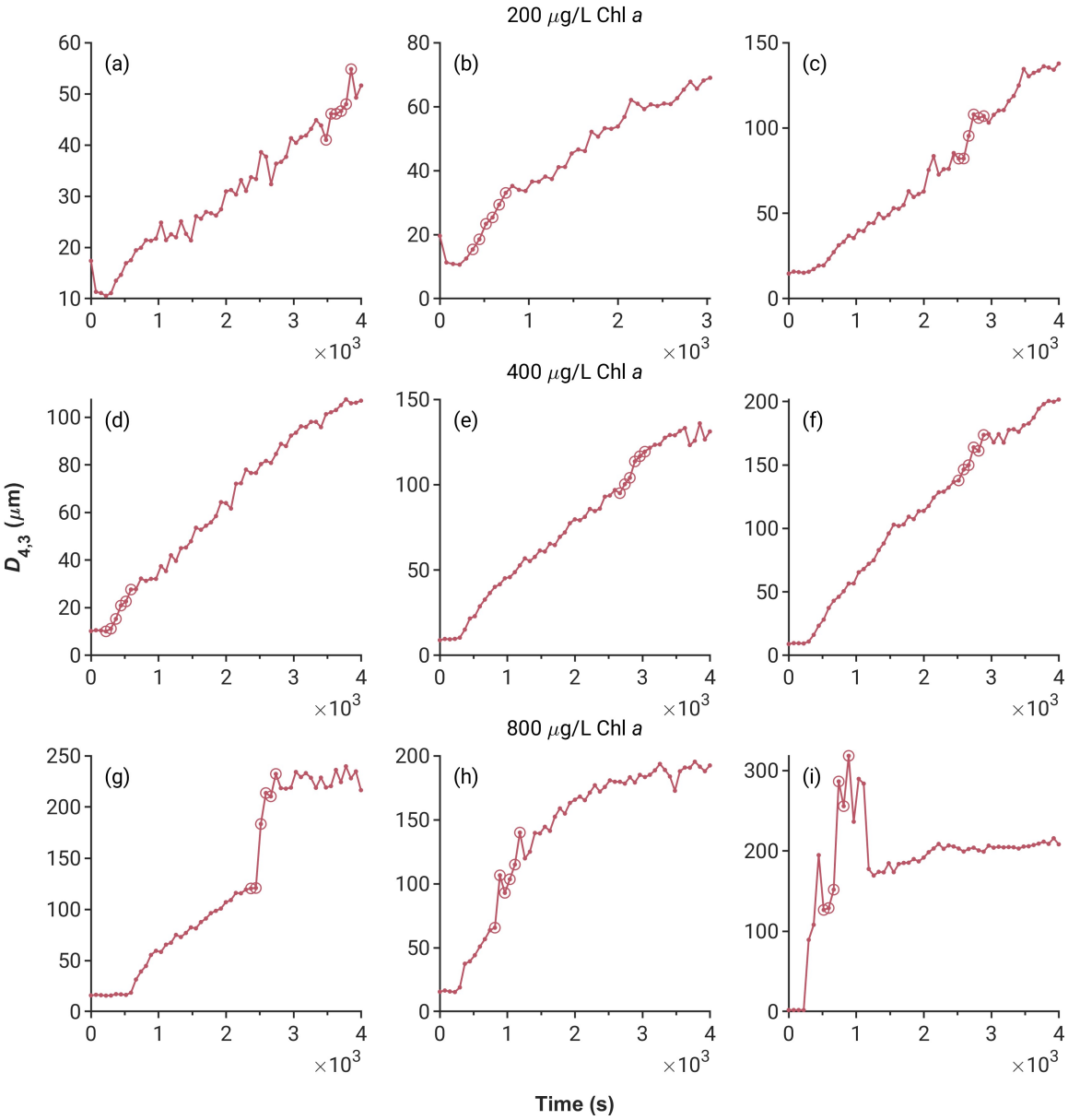

Fig. S10: Time evolution of $D_{4,3}$ of flocs in *M. aeruginosa* cell suspensions in the presence of alum. Top row: 200 μg/L Chl *a*. Middle row: 400 μg/L Chl *a*. Bottom row: 800 μg/L Chl *a*. Left column: 0.1 g/L alum. Center column: 0.2 g/L alum. Right column: 0.4 g/L alum. Circled points indicate the region of maximum local rate of rise in $D_{4,3}$.

S7 Floc size evolution of *M. aeruginosa* with *M. oleifera*

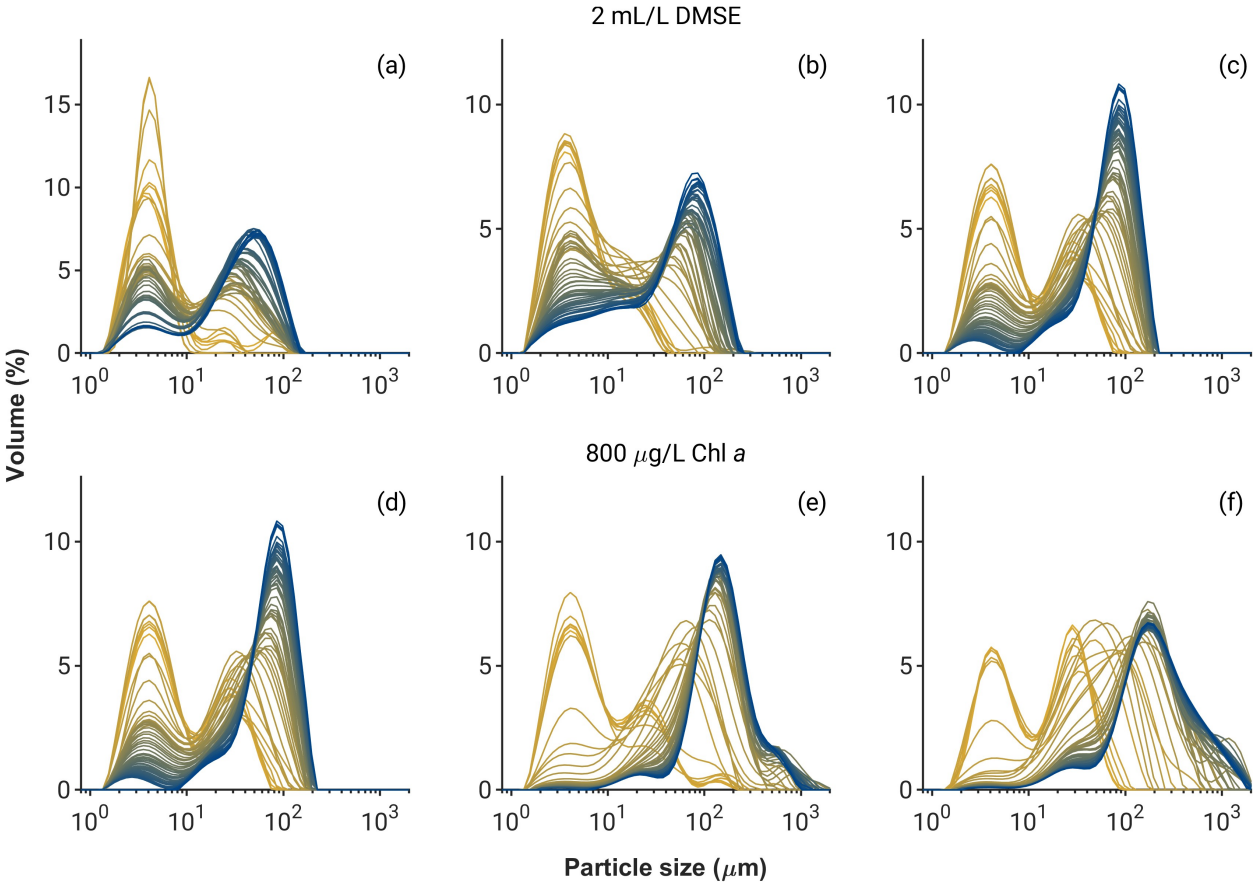

Fig. S11: Time evolution of floc volume distribution in *M. aeruginosa* cell suspensions. Top row: 2 mL/L DMSE with cell densities of 200, 400, and 800 μg/L Chl *a* (left to right). Bottom row: *M. aeruginosa* at 800 μg/L Chl *a*, with DMSE concentrations of 2, 6, and 8 mL/L (left to right). Measurements taken approximately every 74 s. Stirring speed = 70 rpm.

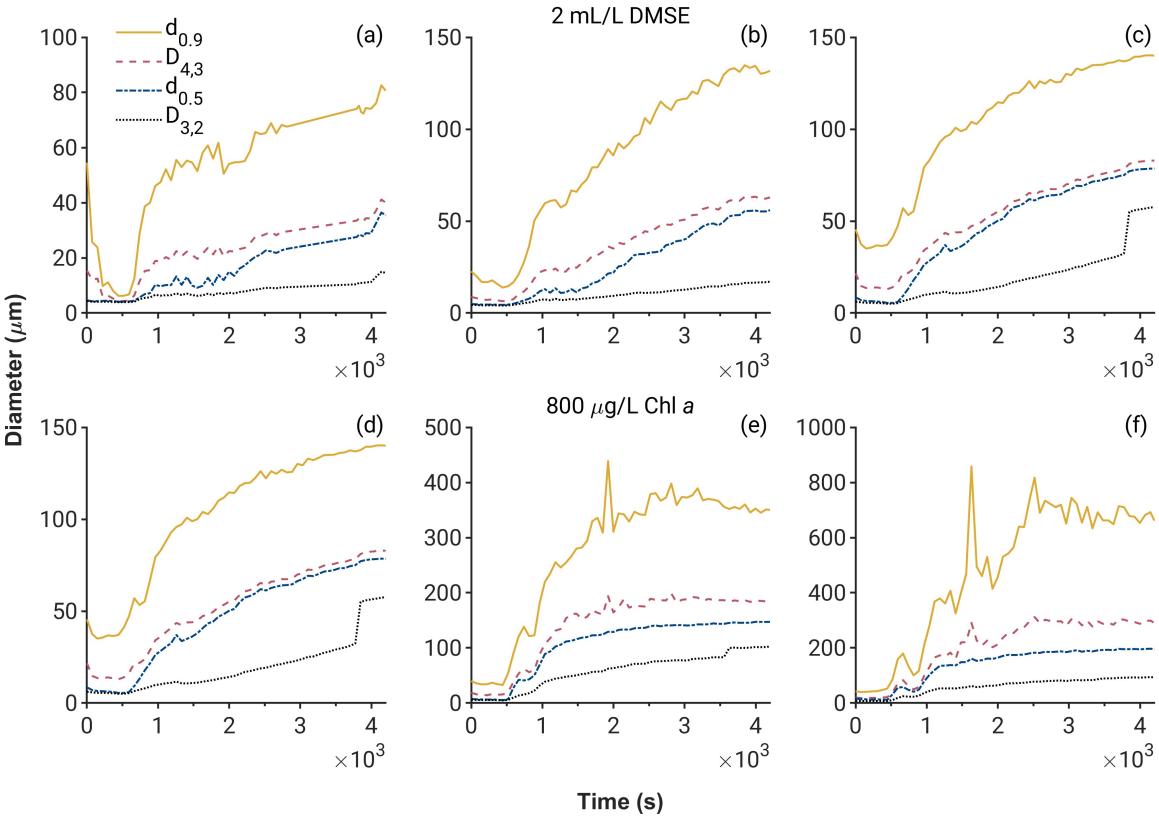

Fig. S12: Time evolution of floc diameters in *M. aeruginosa* cell suspensions. Top row: 2 mL/L DMSE with cell densities of 200, 400, and 800 μg/L Chl *a* (left to right). Bottom row: *M. aeruginosa* at 800 μg/L Chl *a*, with DMSE concentrations of 2, 6, and 8 mL/L (left to right). Measurements taken approximately every 74 s. Stirring speed = 70 rpm.

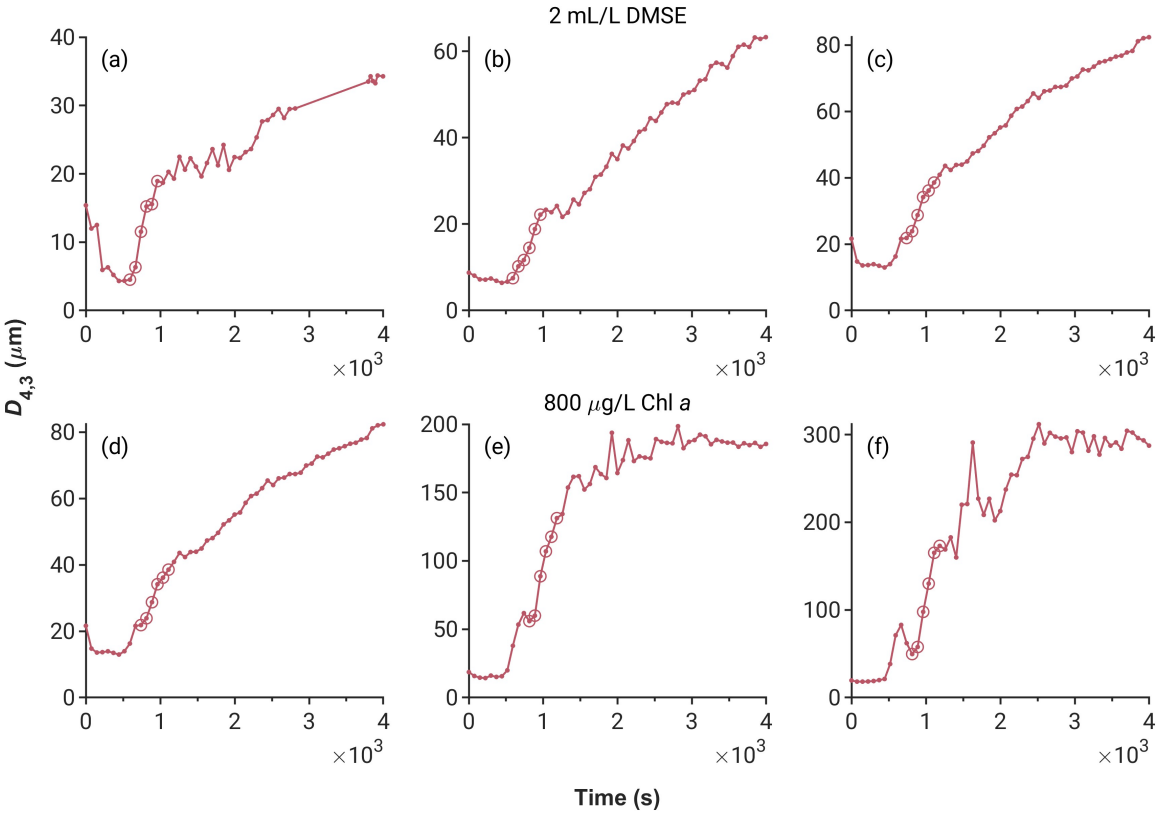

Fig. S13: Time evolution of $D_{4,3}$ of *M. aeruginosa* cell suspensions. Top row: 2 mL/L DMSE with cell densities of 200, 400, and 800 μg/L Chl *a* (left to right). Bottom row: *M. aeruginosa* at 800 μg/L Chl *a*, with DMSE concentrations of 2, 6, and 8 mL/L (left to right). Circled points indicate the region of maximum local rate of rise in $D_{4,3}$.

S8 Temporal profiles of fractal dimension

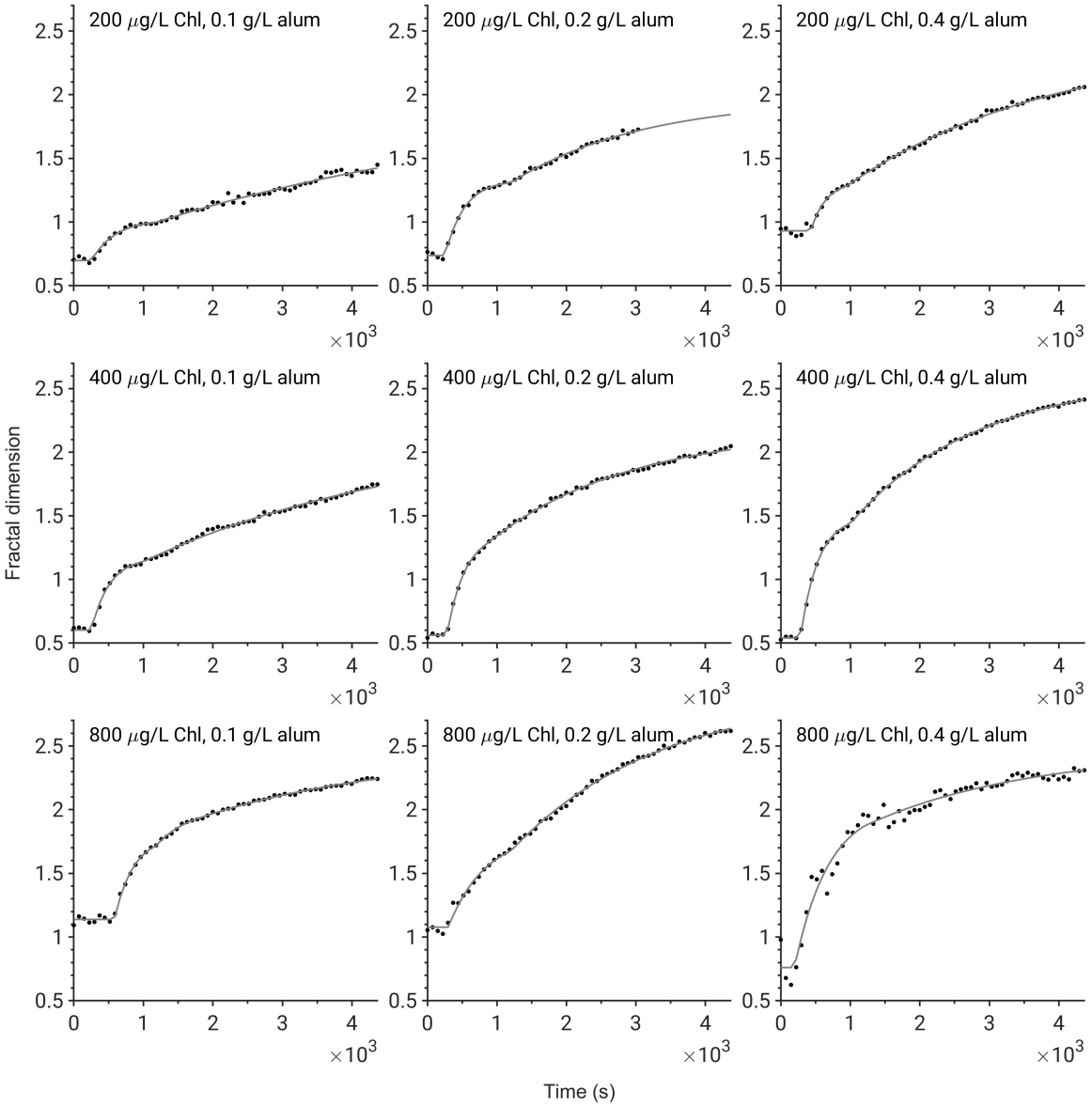

Fig. S14: Evolution of fractal dimension of *M. aeruginosa* flocs during alum-induced flocculation.

Fig. S14 shows the evolution of the fractal dimension in the flocculation of *M. aeruginosa* using alum. The symbols are experimental data, and the curves represent the fit of the data to the mathematical model in eqn (S3). This model is based on a first-order rate of increase [eqn (6) of the main article] and includes a delay time, t_0, to account for the induction period observed at the start of the measurements. In most experiments with alum, an initial rapid increase to a certain low fractal dimension, $d_{\mathrm{F},1}$, was followed by a slower restructuring to a higher value, $d_{\mathrm{F,max}}$. Therefore, the model incorporates two rate constants, k_1 and k_2,

corresponding to these two phases. Fig. S15 shows the fractal dimension evolution profiles for experiments using DMSE.

$$d_{\mathrm{F}} = \begin{cases} d_{\mathrm{F},0}, & \text{for } t \le t_0 \\ d_{\mathrm{F},1} - \left(d_{\mathrm{F},1} - d_{\mathrm{F},0}\right) \exp\left[-k_1 \left(t - t_0\right)\right], & \text{for } t_0 < t \le t_1 \\ d_{\mathrm{F,max}} - \left(d_{\mathrm{F,max}} - d_{\mathrm{F},1}\right) \exp\left[-k_2 \left(t - t_1\right)\right], & \text{for } t > t_1 \end{cases} \tag{S3}$$

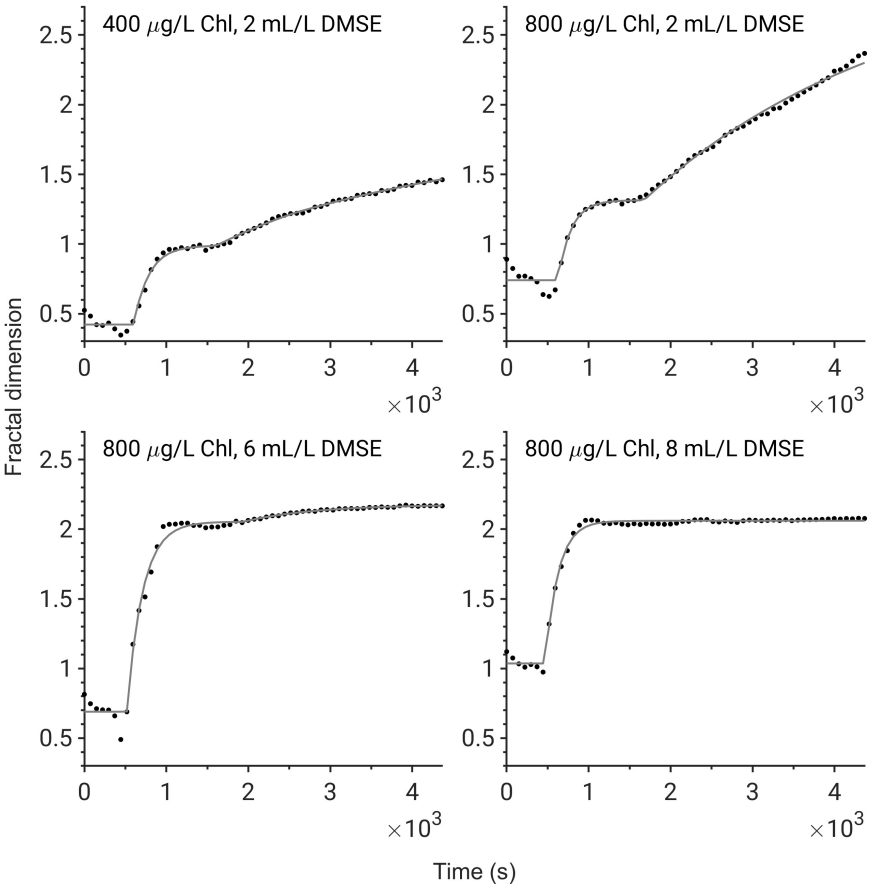

Fig. S15: Evolution of fractal dimension of *M. aeruginosa* flocs during flocculation induced by *M. oleifera*.

References

(1) U. Gassenschmidt, K. D. Jany, T. Bernhard and H. Niebergall, *Biochimica et Biophysica Acta*, 1995, **1243**, 477–481.

(2) J. E. C. Freire, I. M. Vasconcelos, F. B. M. B. Moreno, A. B. Batista, M. D. P. Lobo, M. L. Pereira, J. P. M. S. Lima, R. V. M. Almeida, A. J. S. Sousa, A. C. O. Monteiro-Moreira, J. T. A. Oliveira and T. B. Grangeiro, *PLOS ONE*, 2015, **10**, 1–24.

(3) A. Ndabigengesere and K. S. Narasiah, *Water Research*, 1998, **32**, 781–791.

(4) M. M. Özcan, *South African Journal of Botany*, 2020, **129**, 25–31.

(5) A. Ndabigengesere, K. S. Narasiah and B. G. Talbot, *Water Research*, 1995, **29**, 703–710.

(6) K. A. Ghebremichael, K. Gunaratna, H. Henriksson, H. Brumer and G. Dalhammar, *Water Research*, 2005, **39**, 2338–2344.

(7) A. Jain, R. Subramanian, B. Manohar and C. Radha, *Journal of Food Science and Technology*, 2019, **56**, 2093–2104.

(8) N. A. Oladoja and G. Pan, *Sustainable Chemistry and Pharmacy*, 2015, **2**, 37–43.

(9) F. P. Camacho, V. S. Sousa, R. Bergamasco and M. Ribau Teixeira, *Chemical Engineering Journal*, 2017, **313**, 226–237.

(10) G. S. Madrona, G. B. Serpelloni, A. M. Salcedo Vieira, L. Nishi, K. C. Cardoso and R. Bergamasco, *Water, Air, & Soil Pollution*, 2010, **211**, 409–415.

(11) T. Okuda, A. U. Baes, W. Nishijima and M. Okada, *Water Research*, 1999, **33**, 3373–3378.

(12) Pierce Biotechnoloy, *Pierce Biotechnology Technical Resource, TR0006.0: Extinction Coefficients*, 2002.

(13) *Mastersizer 2000 User Manual, Malvern Instruments*, 2007.